FGF signaling regulates mesenchymal differentiation and skeletal patterning along the limb bud proximodistal axis

Kai Yu and David M. Ornitz*

Fibroblast growth factors (FGFs) are signals from the apical ectodermal ridge (AER) that are essential for limb pattern formation along the proximodistal (PD) axis. However, how patterning along the PD axis is regulated by AER-FGF signals remains controversial. To further explore the molecular mechanism of FGF functions during limb development, we conditionally inactivated fgf receptor 2 (*Fgfr2*) in the mouse AER to terminate all AER functions; for comparison, we inactivated both *Fgfr1* and *Fgfr2* in limb mesenchyme to block mesenchymal AER-FGF signaling. We also re-examined published data in which *Fgf4* and *Fgf8* were inactivated in the AER. We conclude that limb skeletal phenotypes resulting from loss of AER-FGF signals cannot simply be a consequence of excessive mesenchymal cell death, as suggested by previous studies, but also must be a consequence of reduced mesenchymal proliferation and a failure of mesenchymal differentiation, which occur following loss of both *Fgf4* and *Fgf8*. We further conclude that chondrogenic primordia formation, marked by initial *Sox9* expression in limb mesenchyme, is an essential component of the PD patterning process and that a key role for AER-FGF signaling is to facilitate SOX9 function and to ensure progressive establishment of chondrogenic primordia along the PD axis.

KEY WORDS: FGF, FGF receptor, Apical ectodermal ridge (AER), Limb bud development, Chondrogenesis

INTRODUCTION

The apical ectodermal ridge (AER) is a specialized ectodermal structure formed at the distal tip of the vertebrate limb bud that is essential for proximodistal (PD) patterning of the limb (Saunders, 1948). Surgical removal of the AER results in skeletal truncation that is limited to more distal segments when the AER is removed at progressively later stages (Rowe and Fallon, 1982; Summerbell, 1974). The AER functions by elaborating signals to the adjacent mesenchyme, and members of the fibroblast growth factor (FGF) family have been identified as key components of AER signaling (Martin, 1998). It has been demonstrated that FGF-soaked beads are sufficient to rescue the skeletal phenotypes that result from AER removal (Fallon et al., 1994; Niswander et al., 1993). Of the four FGFs expressed in the AER, *Fgf4* and *Fgf8* are necessary for limb skeletal formation and when both genes are disrupted prior to limb bud initiation, the entire limb skeleton fails to form (Boulet et al., 2004; Sun et al., 2002).

FGFs elicit their biological functions by binding and activating a family of four high-affinity receptors (FGFRs), a sub-class of receptor tyrosine kinases (Ornitz and Itoh, 2001; Zhang et al., 2006). Two members of the FGFR family, *Fgfr1c* and *Fgfr2c*, are expressed in nascent limb bud mesenchyme (Orr-Urtreger et al., 1991). In vitro studies demonstrate that both FGFR1c and FGFR2c are capable of interacting with AER-expressed FGFs (Ornitz et al., 1996; Zhang et al., 2006). After ligand binding, activated FGFRs trigger several downstream intracellular signaling cascades (Eswarakumar et al., 2005). During limb development, the MAP kinase signaling pathway is activated in mesenchymal cells immediately adjacent to the AER, indicating active AER-FGF signaling in distal limb mesenchyme (Corson et al., 2003).

Previous studies indicate that AER-FGF signals are important for maintaining mesenchymal cell survival during limb development (Boulet et al., 2004; Sun et al., 2002). However, although AER-FGF signals are limited to distal mesenchyme, cell death induced by loss of AER-FGFs appears in proximal mesenchyme, far away from the AER. This is inconsistent with current knowledge that FGFs act as paracrine factors due to their interaction with heparan sulfate proteoglycans (HSPGs) in the extracellular matrix (ECM) (Ornitz, 2000). Moreover, when *Fgf4* and *Fgf8* are disrupted after limb bud initiation, transient AER-FGF signaling allows formation of a severely hypoplastic skeleton (Sun et al., 2002). Notably, despite significant size and number reduction of skeletal elements, all three PD segments are still recognizable. By contrast, AER removal, after limb bud initiation, results in a truncated skeleton owing to loss of all skeletal elements in distal segments. Phenotypic differences between loss of the AER and loss of AER-FGFs suggest that the AER possesses additional functions, which are either not mediated by FGF4 and FGF8 or are redundantly mediated by other AER factors such as FGF9, FGF17, or other signaling molecules including WNTs and BMPs (Barrow et al., 2003; Wang et al., 2004; Yamaguchi et al., 1999). All of these phenotypes, which undoubtedly have mechanistic implications, are not readily explained by the current model(s) of AER-FGF functions during limb development.

To further understand the functions of AER-FGF signals during limb development, we used a genetic analysis in the mouse embryo to compare phenotypes resulting from loss of the AER with phenotypes resulting from loss of AER-FGF signals. We also compared phenotypes resulting from partial loss of AER-FGF signaling with phenotypes resulting from complete loss of both *Fgf4* and *Fgf8* in the AER. We conclude that AER-FGF signals regulate multiple molecular and cellular processes during limb development and that the skeletal agenesis after complete loss of both *Fgf4* and *Fgf8* is due to combined mesenchymal defects, including increased cell death, decreased proliferation and failure of chondrogenic differentiation. We present a model to explain how AER-controlled

Department of Developmental Biology, Washington University School of Medicine, St Louis, MO 63110 USA.

*Author for correspondence (e-mail: dornitz@wustl.edu)

proliferation and FGF-regulated mesenchymal differentiation organize the formation of the skeletal primordia along the PD axis during normal limb development.

MATERIALS AND METHODS

Mice

Sources: $Fgfr1^{flox/+}$ and $Fgfr1^{\Delta/+}$ (Trokovic et al., 2003); $Fgfr2^{flox/flox}$ and $Fgfr2^{\Delta/+}$ (Yu et al., 2003); $Msx2$-Cre (Sun et al., 2000); $Prx1$-Cre (Logan et al., 2002). $Fgfr2^{Msx2-Cre}$ mice were generated by mating $Fgfr2^{+/\Delta}$; $Msx2^{Cre/+}$ mice with $Fgfr2^{flox/flox}$ mice. $Fgfr1^{Prx1-Cre}$, $Fgfr2^{Prx1-Cre}$ and $Fgfr1/2^{Prx1-Cre}$ mice were generated by mating $Fgfr1^{+/\Delta}$; $Fgfr2^{+/\Delta}$; $Prx1^{Cre/+}$ compound heterozygous mice with $Fgfr1^{flox/flox}$; $Fgfr2^{flox/flox}$ double homozygous mice. In all matings, $Fgfr1^{\Delta}$ and $Fgfr2^{\Delta}$ alleles were incorporated to increase the efficiency of Cre-mediated recombination. Mouse embryonic skeletons were prepared as described previously (Yu et al., 2003).

Staining, immunohistochemistry and in situ hybridization

Embryos or tissues were fixed in 4% paraformaldehyde in PBS and embedded in paraffin. Sections were stained with Hematoxylin and Eosin (H&E). For β-galactosidase histochemistry, embryos were fixed in 0.2% glutaraldehyde in PBS for 60 minutes, washed in PBS and stained in β-gal staining buffer [5 mM $K_3Fe (CN)_6$, 5 mM $K_4FE (CN)_6 \cdot 3H_2O$, 1 mM $MgCl_2$, 0.01% sodium desoxycholate, 0.009% NP40, 0.002% X-Gal] for 8 hours at 4°C. After post-fixing in 4% paraformaldehyde, embryos were embedded in paraffin and sections counterstained with nuclear fast red.

Immunohistochemistry was carried out using LAB-SA Detection System (Zymed) according to the manufacturer's instructions. Primary antibodies are anti-cleaved caspase 3 (Cell Signaling) and anti-phosphohistone H3 (pHH3) (Sigma). TUNEL assay was carried out using the In Situ Cell Death Detection Kit (Roche) according to the manufacturer's instructions. Distal mesenchymal proliferation was analyzed on transverse sections of limb buds and pHH3-labeled mesenchymal cells were counted in a 1.5×10^4 μm^2 area immediately adjacent (within 100 μm) to the AER.

$Fgf8$ whole-mount in situ hybridization was performed as described previously (Sun et al., 2000).

RESULTS

AER ablation by conditional removal of $Fgfr2$ in limb ectoderm

To understand functional differences between the AER and AER-FGFs, we ablated the AER in mouse limb buds, which allowed us to directly compare phenotypes with those resulting from inactivation of $Fgf4$ and $Fgf8$ in the AER. Because $Fgfr2b$ is essential for the survival of AER epithelial cells (Revest et al., 2001), conditional inactivation of $Fgfr2$, using the limb ectoderm-specific $Msx2$-Cre transgene (Sun et al., 2000), could be used to terminate AER functions during limb development. $Msx2$-$Cre/+$; $Fgfr2^{flox/\Delta}$ ($Fgfr2^{Msx2-Cre}$) mice appeared normal except for the absence of hindlimbs and severely truncated forelimbs (Fig. 1A-F), consistent with expression of $Msx2$-Cre before hindlimb bud initiation and after forelimb bud initiation (Lewandoski et al., 2000). $Fgfr2^{Msx2-Cre}$ forelimbs formed a normal stylopod (humerus) and zeugopod (radius and ulna), but completely lacked an autopod (Fig. 1D,E). The mutant forelimb skeleton was very similar to the truncated chicken wing skeleton that results from AER removal at around stage 23 (Summerbell, 1974), indicating that genetic methods can mimic the effects of surgical means to completely ablate the AER during limb development.

In $Fgfr2^{Msx2-Cre}$ mice, forelimb buds were initiated normally, but showed reduced distal outgrowth after embryonic day 10.5 (E10.5). By E11.5, mutant forelimb buds were only comparable in size to control limb buds at E10.5 and showed distal morphological deformities (Fig. 1R, dotted line). By E12.5, mutant forelimbs appeared truncated, lacking any autopod primordial structures (Fig.
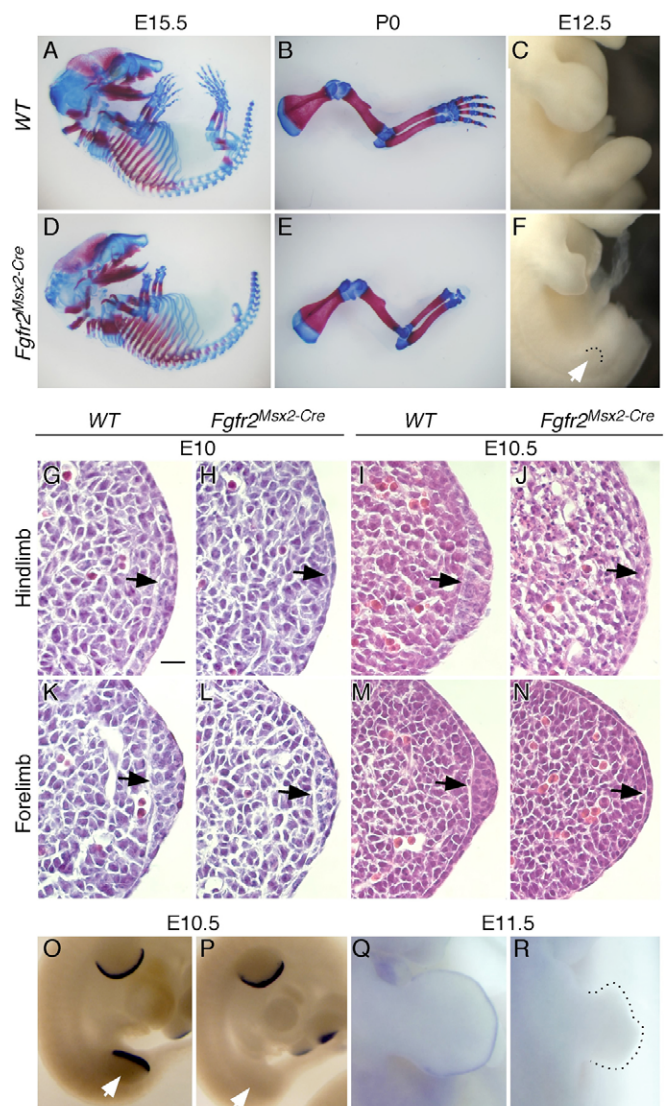
Fig. 1. Limb development phenotypes in $Fgfr2^{Msx2-Cre}$ mouse embryos. (**A-F**) Comparison of limb phenotypes in wild-type control (WT) and $Fgfr2^{Msx2-Cre}$ mouse embryos. (A,D) Skeletal preparations of E15.5 embryos. (B,E) Skeletal preparations of P0 forelimbs. (C,F) Gross appearance of limb buds at E12.5. Note that the hindlimb bud is never formed and only appears as a small bulge (arrow and dotted line) in $Fgfr2^{Msx2-Cre}$ embryos. (**G-J**) Histology of the distal hindlimb buds at E10 (G,H) and E10.5 (I,J) showing the failure to form a multi-layered AER (arrow) in $Fgfr2^{Msx2-Cre}$ embryos. (**K-N**) Histology of the distal forelimb buds at E10 (K,L) and E10.5 (M,N) showing initial formation of an AER (arrow) in $Fgfr2^{Msx2-Cre}$ embryos at E10 and regression to a single-layered epithelium by E10.5. (**O-R**) Whole-mount in situ hybridization showing $Fgf8$ expression in the AER at E10.5 (O,P) and E11.5 (Q,R). Note that $Fgf8$ is never expressed in $Fgfr2^{Msx2-Cre}$ hindlimbs (arrow) and is prematurely lost in $Fgfr2^{Msx2-Cre}$ forelimbs, accompanied by distal deformities (dotted line). Data are representative of at least three embryos. Scale bar: in G for G-N, 20 μm.

1C,F). By contrast, mutant hindlimbs only developed a small bulge protruding from the body wall and never demonstrated further outgrowth (Fig. 1F, arrow and dotted line).

Examination of histological sections indicated that a stratified AER was never formed in $Fgfr2^{Msx2-Cre}$ hindlimb buds (Fig. 1G-J). Consistent with agenesis of the AER in mutant hindlimbs, $Fgf8$ was
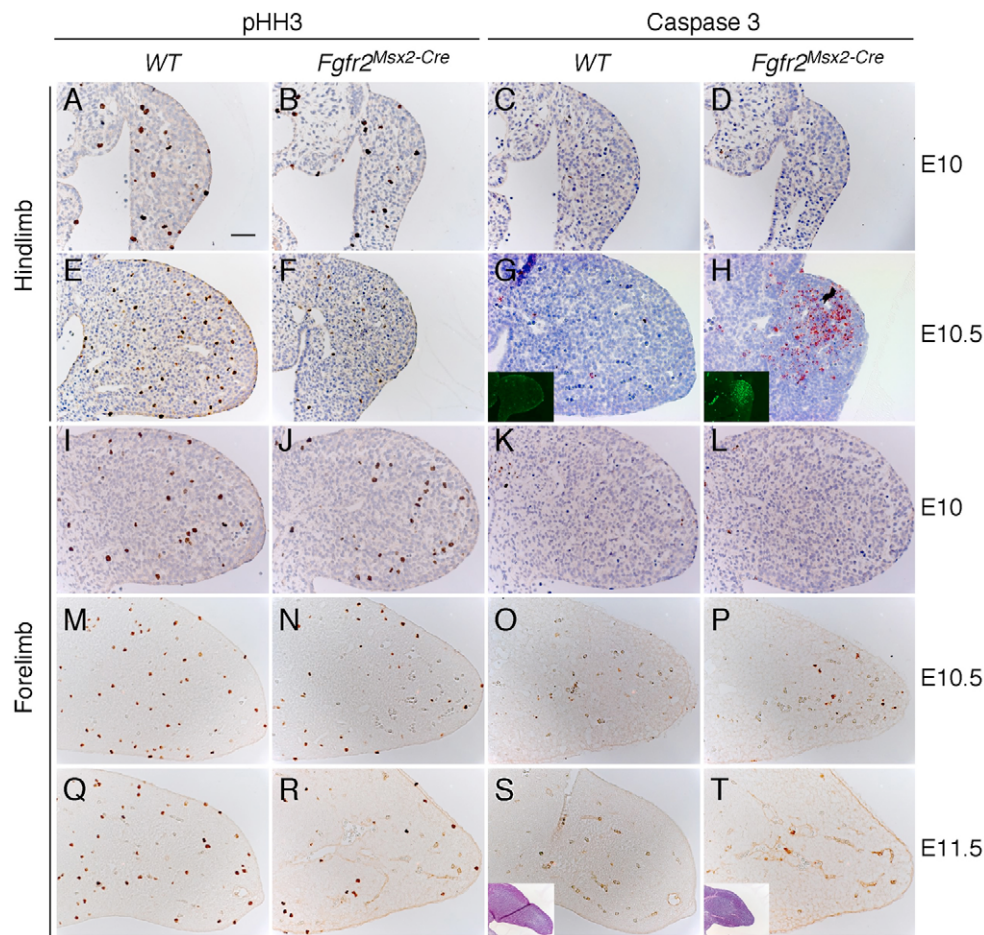
Fig. 2. Reduced mesenchymal proliferation and increased cell death after loss of the AER in *Fgfr2^Msx2-Cre* mouse embryos. Phosphohistone H3 (pHH3) immunohistochemistry was used to assess mesenchymal proliferation. Caspase 3 immunohistochemistry and TUNEL assay were used to assess cell death. Hindlimb (**A-H**) and forelimb (**I-T**) sections are shown at the developmental times indicated. Insets in G and H show TUNEL labeling on adjacent sections. Insets in S and T show the overall size of the limb buds at E11.5. Data are representative of at least three embryos. Scale bar: 50 µm.

not detected at any stage examined (Fig. 1O,P and data not shown). In mutant forelimbs, transient epithelial thickening was observed in the prospective AER region at E10, which rapidly regressed to a single layer of epithelial cells by E10.5 (Fig. 1K-N). *Fgf8* expression was detected in the AER at E10.5, but was prematurely lost by E11.5 (Fig. 1O-R).

In a previous study, conditional disruption of *β-catenin* (*Ctnnb1* – Mouse Genome Informatics) in the AER with *Msx2-Cre* (*β-catenin^Msx2-Cre*) resulted in hindlimb skeletal agenesis that was indistinguishable from the hindlimb phenotypes of *Fgfr2^Msx2-Cre* mice. However, *β-catenin^Msx2-Cre* mice showed significantly more severe forelimb phenotypes than *Fgfr2^Msx2-Cre* mice, with skeletal truncation occurring at the elbow joint level rather than at the wrist level (Barrow et al., 2003). As the truncation level correlates with the timing of AER removal in chick experiments, these results indicate that AER functions are lost at a later stage in *Fgfr2^Msx2-Cre* forelimbs than in *β-catenin^Msx2-Cre* forelimbs. Since the same *Msx2-Cre* transgene was used in both studies, it suggests that AER ablation in the forelimbs is not determined by the time of gene targeting but more likely by the time of protein inactivation.

The AER is essential for proliferation of adjacent limb mesenchyme

Previous studies indicated that AER extirpation results in reduced proliferation and/or increased cell death in distal mesenchyme (Dudley et al., 2002; Niswander and Martin, 1993; Rowe et al., 1982; Sun et al., 2002). Mesenchymal proliferation and cell death were examined in *Fgfr2^Msx2-Cre* limb buds using anti-phosphohistone

H3 (pHH3) and anti-caspase 3 immunohistochemistry (IHC), respectively. Consistent with the complete absence of AER functions, mutant hindlimb buds showed decreased mesenchymal proliferation beginning at the limb bud initiation stage (E10) (Fig. 2A,B; Table 1). By E10.5, mesenchymal proliferation was further decreased in mutant limb mesenchyme, and few pHH3-positive cells were found throughout the whole hindlimb field (Fig. 2E,F; Table 1). In contrast to the reduced proliferation observed at early stages, mesenchymal cell death did not appear in the hindlimb buds until E10.5, when massive cell death was detected throughout the entire limb mesenchyme, adjacent to the prospective AER (Fig. 2C,D,G,H; Table 1). Mutant forelimbs showed normal mesenchymal proliferation at E10 (Fig. 2I,J; Table 1). However, by E10.5, reduced proliferation was evident in distal mesenchyme (Fig. 2M,N; Table 1). At E11.5, mutant forelimb buds lacked highly proliferative distal mesenchyme (Fig. 2Q,R). No abnormal mesenchymal cell death was found in mutant forelimbs at E10 (Fig. 2K,L). At E10.5, mutant forelimbs showed a slight increase in cell death in distal mesenchyme (Fig. 2O,P; Table 1). At E11.5, apoptotic cells were no longer detected in distal mesenchyme (Fig. 2S,T). This is consistent with the reduced or absent cell death observed after AER extirpation at later stages of chick limb development (Dudley et al., 2002; Rowe et al., 1982), further indicating that loss of AER functions occurs at a later developmental stage in *Fgfr2^Msx2-Cre* forelimbs.

Comparison of *Msx2-Cre*, *Fgf4/8* double conditional knockout (*Fgf4/8^Msx2-Cre*) mice (Sun et al., 2002), which do not show reduced distal mesenchymal proliferation at early stages, with *Fgfr2^Msx2-Cre* mice, revealed that either the AER contributes to mesenchymal

Table 1. Limb bud mesenchymal proliferation and cell death

	E10			E10.5		
	WT	$Fgfr2^{Msx2-Cre}$	$Fgfr1/2^{Prx1-Cre}$	WT	$Fgfr2^{Msx2-Cre}$	$Fgfr1/2^{Prx1-Cre}$
pHH3						
Forelimb	7.1 (21)	6.8 (15)	6.9 (19)	7.7 (20)	5.8 (24)	8.4 (13)
s.d.	2.7	2.3	2.1	2.0	2.0	2.5
P value		NS	NS		0.003	NS
Hindlimb	6.0 (16)	4.6 (18)		6.8 (5)	4.0 (5)	
s.d.	1.3	1.8		1.3	1.2	
P value		0.011			0.008	
Caspase 3						
Forelimb	–/+	–/+	++	–/+	+	–/+
Hindlimb	–/+	–/+		–/+	+++	

Shown are the average number of phosphohistone H3 (pHH3)-labeled cells in a 1.5×10^4 μm^2 area adjacent to the AER, with the number of sections examined from at least three embryos in parentheses. Low frequency of caspase 3 (or TUNEL, not shown)-positive cells (–/+); transient proximal cell death (++); slightly increased distal mesenchymal cell death (+); cell death throughout the entire limb bud mesenchyme (+++).
NS, Not significantly different from wild type (WT).

proliferation independently of FGF4 and FGF8, or that mesenchymal proliferation is redundantly regulated by these FGFs and other AER signals. As pointed out in previous studies (Sun et al., 2002), it is puzzling that in $Fgf4/8^{Msx2-Cre}$ limb buds, the cell-death zone is located in proximal mesenchyme, whereas AER removal leads to cell death in distal mesenchyme. However, what was not rigorously considered during such a comparison was whether loss of all AER functions versus loss of AER-FGFs happens at the same developmental stages. As demonstrated in previous studies, removal of the AER at different times can lead to different mesenchymal defects and skeletal phenotypes (Dudley et al., 2002). Thus, to understand functional differences between the AER and AER-FGFs, it is necessary to choose and compare phenotypes that occur at the same stages of development. Hindlimb phenotypes of $Fgfr2^{Msx2-Cre}$ mice and $Fgf4/8^{Msx2-Cre}$ mice allow such a comparison. $Fgf8$, which is expressed before limb bud initiation, mediates AER-like functions before formation of a morphologically identifiable AER. In $Fgfr2^{Msx2-Cre}$ hindlimbs, $Fgf8$ was never expressed, similar to the situation for $Fgf4/8^{Msx2-Cre}$ hindlimbs, but, additionally, the AER was never formed. By contrast, a morphologically normal AER is present in $Fgf4/8^{Msx2-Cre}$ hindlimbs at early stages (Sun et al., 2002). Thus, it is conceivable that before or during limb bud initiation, all AER functions are lost in $Fgfr2^{Msx2-Cre}$ hindlimbs, whereas only FGF signals are lost in $Fgf4/8^{Msx2-Cre}$ hindlimbs. However, despite the loss of all AER-derived signals, mesenchymal cell death in $Fgfr2^{Msx2-Cre}$ hindlimbs occurs at the same time as that of $Fgf4/8^{Msx2-Cre}$ hindlimbs (35 somites, E10.5), strongly suggesting that the survival function of the AER is solely mediated by FGF signals. Phenotypic comparison of $Fgf4/8^{Msx2-Cre}$ and $Fgfr2^{Msx2-Cre}$ hindlimbs also suggests that the proximal location of the cell-death domain, after loss of AER-FGF signals, is likely to be due to continued proliferation of distal mesenchyme, which is not affected by loss of AER-FGF signals at early stages (Sun et al., 2002). As apoptosis is delayed, continual proliferation gradually separates dying mesenchymal cells from the AER. Without distal mesenchymal proliferation, the same cell-death domain will remain adjacent to the ectoderm/AER, as shown in $Fgfr2^{Msx2-Cre}$ hindlimbs (Fig. 2H).

FGFR1 and FGFR2 mediate AER-FGF signaling during early limb development

To further understand the mechanism of AER-FGF functions, we disrupted FGF signal transduction in limb mesenchyme by targeting mesenchymal FGFRs. To overcome potential functional redundancy between $Fgfr1c$ and $Fgfr2c$, we inactivated both $Fgfr1$ and $Fgfr2$ in limb mesenchyme with a $Prx1-Cre$ transgene ($Prx1$ is also known as $Prrx1$ – Mouse Genome Informatics) (Logan et al., 2002). $Prx1-Cre$ is expressed in both forelimb and hindlimb mesenchyme, but is activated in the prospective forelimb region prior to limb bud initiation and targets forelimb mesenchyme exclusively at initiation stages of limb bud development (Fig. 3A). Double conditional knockout mice with the genotype $Prx1-Cre/+;$ $Fgfr1^{flox/\Delta}; Fgfr2^{flox/\Delta}$ ($Fgfr1/2^{Prx1-Cre}$) were born alive along with compound single conditional knockout littermates, $Fgfr1^{Prx1-Cre}$ ($Prx1-Cre/+; Fgfr1^{flox/\Delta}; Fgfr2^{flox/+}$) and $Fgfr2^{Prx1-Cre}$ ($Prx1-Cre/+; Fgfr1^{flox/+}; Fgfr2^{flox/\Delta}$). $Fgfr1^{Prx1-Cre}$ mice showed mild limb-skeletal defects (Fig. 3B,C and see Fig. S1 in the supplementary material) and $Fgfr2^{Prx1-Cre}$ skeletons were indistinguishable from wild-type skeletons at post-natal day 0 (P0) (data not shown), consistent with previous findings (Eswarakumar et al., 2002; Li et al., 2005; Verheyden et al., 2005; Yu et al., 2003). In contrast to the single-gene knockouts, $Fgfr1/2^{Prx1-Cre}$ mice showed severe skeletal hypoplasia in both forelimbs and hindlimbs (Fig. 3B,D and see Fig. S1 in the supplementary material). All three segments of the forelimb skeleton were severely affected and bony fusion was found at the elbow joint and between skeletal elements in the autopod. These results suggest that the functions of $Fgfr1$ and $Fgfr2$ are partially redundant during limb skeletal development and that FGFR1 has unique functions in distal limb skeletal formation.

When examined at initiation stages (E9.5), $Fgfr1/2^{Prx1-Cre}$ forelimb buds appeared normal. However, by E10, $Fgfr1/2^{Prx1-Cre}$ forelimb buds were significantly smaller (72%, $P<0.03$) than control limb buds along the PD axis (Fig. 3E,H,I,L; Table 2), a phenotype not found in either $Fgfr1^{Prx1-Cre}$ or $Fgfr2^{Prx1-Cre}$ littermates (Fig. 3E-G,I-K; Table 2). Smaller limb bud size in $Fgfr1/2^{Prx1-Cre}$ embryos could result from decreased mesenchymal cell proliferation or increased cell death. However, proliferation in the distal mesenchyme of $Fgfr1/2^{Prx1-Cre}$ forelimb buds was not affected (Fig. 3M-P), similar to the observations in $Fgf4/8^{Msx2-Cre}$ limb buds (Sun et al., 2002). Increased mesenchymal cell death was not detected in mutant forelimb mesenchyme at E9.5 (25 somites; data not shown); however, at E10 (30-32 somites), increased levels of cell death in $Fgfr1/2^{Prx1-Cre}$ forelimb mesenchyme were clearly present, as shown by caspase 3 IHC (Fig. 3Q,R) and TUNEL labeling (see Fig. S2 in the supplementary material). Apoptotic cells were found in both proximal and central
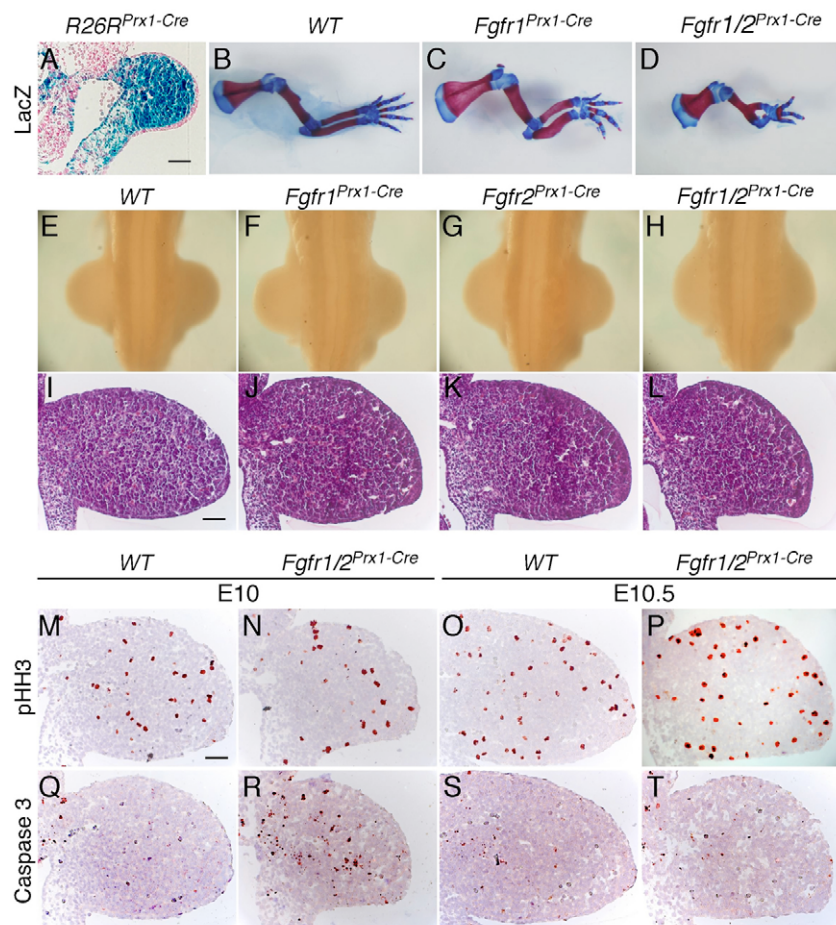
Fig. 3. Limb development phenotypes resulting from FGF receptor inactivation in limb mesenchyme with *Prx1-Cre*. (**A**) β-galactosidase staining of *Prx1-Cre, R26R* forelimb at E9.5. (**B-D**) Skeletal preparations of P0 wild-type control (WT), *Fgfr1^Prx1-Cre^* and *Fgfr1/2^Prx1-Cre^* mice. (**E-L**) Appearance (E-H) and histology (I-L) of E10 forelimb buds of WT, *Fgfr1^Prx1-Cre^*, *Fgfr2^Prx1-Cre^* and *Fgfr1/2^Prx1-Cre^* embryos showing a reduced proximodistal axis in *Fgfr1/2^Prx1-Cre^* forelimb buds. (**M-P**) Phosphohistone H3 (pHH3) immunohistochemistry to assess proliferation at E10 (M,N) and E10.5 (O,P). (**Q-T**) Caspase 3 immunohistochemistry used to assess cell death at E10 (Q,R) and E10.5 (S,T). Note that the region of reduced density of pHH3-positive cells in proximal mesenchyme of *Fgfr1/2^Prx1-Cre^* embryos at E10 (N) corresponds to the region with increased apoptosis (R). Data are representative of at least three embryos. Scale bars: in A, I for I-L and M for M-T, 50 μm.

regions of the limb bud, but were excluded from the most-distal limb mesenchyme. At E10.5, no abnormal cell death was observed in *Fgfr1/2^Prx1-Cre^* forelimbs (Fig. 3S,T). As reported previously, after loss of AER-FGFs, forelimbs show similar mesenchymal defects, including increased proximal cell death and reduced limb bud size, that occur at similar stages of development (E10) (Boulet et al., 2004; Sun et al., 2002), demonstrating that AER-FGF signals are mediated by both FGFR1 and FGFR2 during early mesenchymal development.

When compared with *RAR-Cre* (*RAR* is also known as *Rarb* – Mouse Genome Informatics), *Fgf4/8* double conditional knockout (*Fgf4/8^RAR-Cre^*) forelimbs (Boulet et al., 2004), in which complete loss of FGF4 and FGF8 activity results in skeletal agenesis, *Fgfr1/2^Prx1-Cre^* forelimbs were hypoplastic but formed a normally segmented skeleton. Notably, the *Fgfr1/2^Prx1-Cre^* skeletal phenotype was similar to that of *Fgf4/8^Msx2-Cre^* forelimbs, in which AER-FGF signals are transiently present at early stages. This suggested that in *Fgfr1/2^Prx1-Cre^* forelimbs, early mesenchymal cells still receive FGF signals, albeit at a significantly reduced level. Consistent with this, it has been reported that complete mesenchymal deletion mediated by *Prx1-Cre* may occur by as late as E12.5 (Hill et al., 2006; Kmita et al., 2005; Lewis et al., 2001), suggesting incomplete mesenchymal inactivation of FGFRs by *Prx1-Cre* during early limb development. However, the hypomorphic nature of the *Fgfr1/2^Prx1-Cre^* mutation allows transient FGF signaling, which can then be contrasted with both pre-limb bud initiation and post-limb bud initiation deletions of *Fgf4* and *Fgf8*.

DISCUSSION
Mesenchymal cell death is not sufficient to cause skeletal agenesis
Previous studies concluded that AER-FGF signals regulate limb skeletal formation by maintaining mesenchymal cell survival and, in turn, maintaining the progenitor cell population that will be needed for PD segment formation. After loss of AER-FGF signals, mesenchymal cell death reduces progenitor cell numbers. It has been proposed that skeletal agenesis occurs when progenitor cell numbers fall below some threshold (Boulet et al., 2004; Sun et al., 2002). However, when compared with *Fgf4/8^RAR-Cre^* forelimbs, which completely lack a limb skeleton, both *Fgf4/8^Msx2-Cre^* and *Fgfr1/2^Prx1-Cre^* forelimbs show similar patterns of mesenchymal cell death but they do form a skeleton (Fig. 4B,D,E). It is worth noting that although proximally located cell death domains overlap with the prospective stylopod region, the humerus is the least affected

Table 2. Limb bud proximodistal length

| Somite	n	Fgfr1^Prx1-Cre^	P value	Fgfr1/2^Prx1-Cre^	P value
28	4, –, 4			72*	<0.03
30-31	2, 2, 2	84	NS	74†	<0.02
32-33	4, 6, 4	97	NS	72*	<0.0001

n, Number of limb buds measured (control, *Fgfr1^Prx1-Cre^*, *Fgfr1/2^Prx1-Cre^*); –, not examined.
NS, Not significantly different from wild type (*P*>0.05).
*Proximodistal limb length as percentage of wild-type control.
†Compared to wild-type control and *Fgfr1^Prx1-Cre^* limb buds.

Fig. 4. Comparison of forelimb development and phenotypes derived from genetic studies in the mouse. (**A**) Models for AER-FGF functions in mesenchymal differentiation and chondrogenic primordia formation along the PD axis during normal limb development. *Fgf8* expression in limb field ectoderm at early stages of development stimulates the FGFR-dependent MAP kinase signaling pathway in all mesenchymal cells of the nascent limb bud (red shading) (Corson et al., 2003). Initial *Sox9* expression demarcates the stylopod primordia. Having received AER-FGF signals, these *Sox9*-expressing cells commit to osteochondroprogenitors and will form a mesenchymal condensation. Distal mesenchymal cells, which remain undifferentiated, continue to proliferate under the influence of the AER and receive AER-FGF signals. As *Sox9* expression expands with limb outgrowth, the zeugopod and autopod primordia are sequentially established. (**B-E**) Phenotypes resulting from genetic manipulations of AER-FGF signaling. Loss of AER-FGF signaling does not prevent mesenchymal cells from expressing *Sox9*, but insufficient AER-FGF signaling triggers mesenchymal cell death that leads to skeletal hypoplasia. (B) Attenuated mesenchymal FGF signal transduction achieved by inactivation of *Fgfr1* and *Fgfr2* with the *Prx1-Cre* transgene (see Fig. 3). With progressive *Fgfr* inactivation during early limb bud development, AER-FGF signals are attenuated in limb mesenchyme. Although reduced in size, chondrogenic primordia still form along the PD axis, which leads to a normally segmented but small and dysmorphic skeleton. (C) The *RAR-Cre* transgene results in complete inactivation of *Fgf8* before forelimb bud initiation (Moon and Capecchi, 2000). Without *Fgf8*, mesenchymal cells in the nascent limb bud fail to receive FGF signaling. *Sox9*-expressing cells that are derived from these mesenchymal cells cannot commit to osteochondroprogenitors and fail to form the stylopod primordia. Increased (and precocious) *Fgf4* expression in the AER restores FGF signaling in distal undifferentiated mesenchyme allowing the zeugopod and autopod primordia to sequentially form following *Sox9* expression. (D) The *Msx2-Cre* transgene inactivates *Fgf4* and *Fgf8* after forelimb bud initiation, allowing transient AER-FGF signaling (Sun et al., 2002). Initial FGF signaling in nascent limb mesenchyme ensures stylopod primordia formation. Subsequent loss of *Fgf4* and *Fgf8* impedes

continual commitment of distal mesenchymal cells to osteochondroprogenitors, which is required for formation of normally sized skeletal segments. The severely hypoplastic zeugopod and autopod are formed from small numbers of committed mesenchymal cells that are either derived from nascent limb mesenchyme or result from partial rescue of distal limb mesenchyme by *Fgf9* and *Fgf17*. (E) The *RAR-Cre* transgene results in complete inactivation of *Fgf4* and *Fgf8* before forelimb bud initiation (Boulet et al., 2004). Without AER-FGF signaling, *Sox9*-expressing cells cannot commit to osteochondroprogenitors and fail to form any chondrogenic primordia. Owing to distal mesenchymal defects, the AER or AER functions are not maintained at later stages and distal mesenchymal proliferation is inevitably reduced, which further reduces limb bud size. (**F,G**) Phenotypes resulting from genetic ablation of the AER at different times of limb development. Proliferation in distal mesenchyme or in mesenchyme adjacent to the AER is reduced after loss of the AER, but mesenchymal cell death is manifested only when the AER is disrupted at early stages. (F) Inactivation of *Fgfr2* in the AER after forelimb bud initiation (see Figs 1, 2). AER degeneration results in an arrest of development in distal mesenchyme and autopod primordia fail to form owing to decreased mesenchymal proliferation and loss of the differentiation function of AER-FGFs. Further skeletal development of stylopod and zeugopod primordia, which are established before AER degeneration, is not affected by loss of AER functions at later developmental stages. (G) Inactivation of *Fgfr2b* (Revest et al., 2001) or conditional inactivation of *Fgfr2* in limb field ectoderm before limb bud initiation (in the hindlimb, Figs 1, 2). The absence of any AER function results in decreased mesenchymal proliferation, massive mesenchymal cell death, and subsequent limb bud agenesis. S, stylopod; Z, zeugopod; A, autopod.
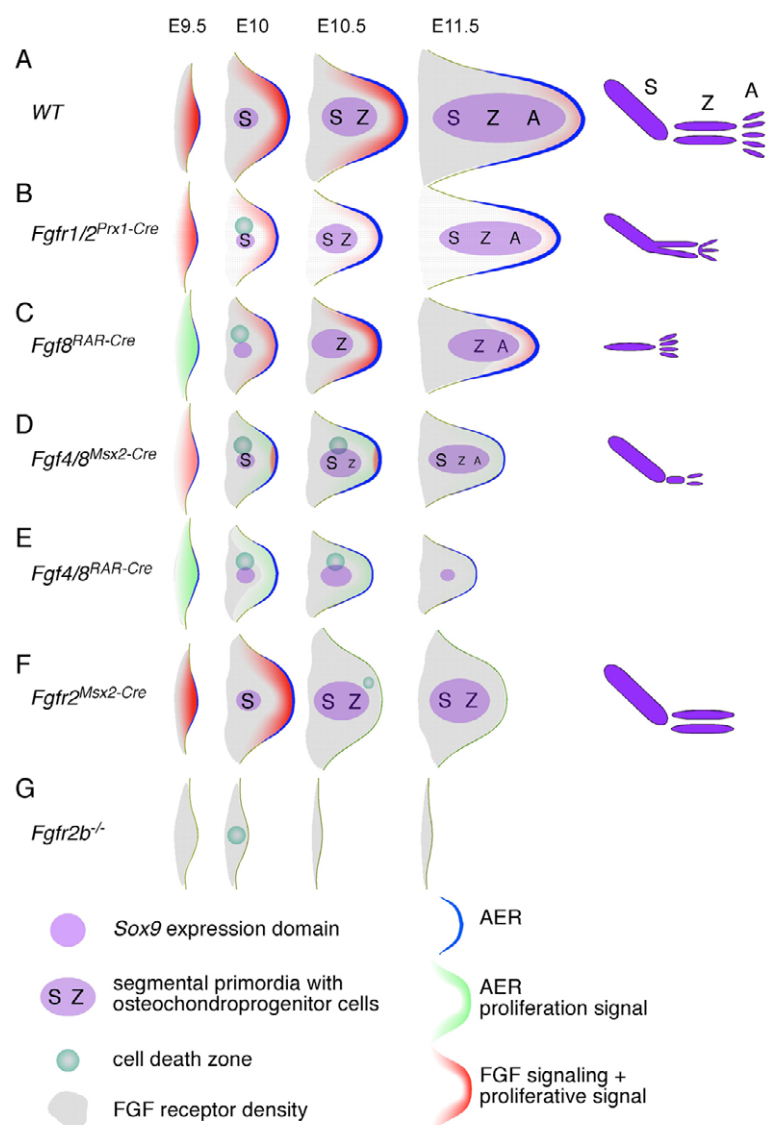
skeletal element in *Fgf4/8^{Msx2-Cre}* forelimbs. These observations suggest that increased mesenchymal cell death is not sufficient to cause skeletal agenesis.

The notion that there is a threshold number of mesenchymal cells to form limb skeletal segments was originally proposed to explain limb PD patterning defects that result from X-irradiation-induced mesenchymal cell death (Wolpert et al., 1979). However,

skeletal defects following X-irradiation are very different from those following loss of both *Fgf4* and *Fgf8*. After X-irradiation, proximal skeletal elements are either not formed or reduced in size, whereas skeletal phenotypes in the autopod are much less severe. It is worth noting that in the X-irradiation model, similar levels of cell death occur in proximal and distal mesenchyme. By contrast, after loss of both *Fgf4* and *Fgf8*, even though

mesenchymal cell death is limited to proximal mesenchyme, distal skeletal elements are either not formed or are severely hypoplastic. As AER functions are not affected by X-irradiation (Wolpert et al., 1979), such phenotypic differences strongly suggest that loss of AER-FGFs must cause additional mesenchymal defects that result in severe distal skeletal phenotypes.

Continual proliferation of distal mesenchyme is essential for distal skeletal formation

Previous studies concluded that skeletal defects, after loss of both *Fgf4* and *Fgf8*, are not due to reduced mesenchymal proliferation, as distal mesenchymal proliferation was not affected by loss of AER-FGF signals when examined before E10.5 (Sun et al., 2002). Although AER-FGF signals are dispensable for mesenchymal proliferation, they are essential to maintain mesenchymal gene expression. One such gene is *Fgf10*, which is abundantly expressed in distal mesenchyme throughout early limb development (Ohuchi et al., 1997). After loss of both *Fgf4* and *Fgf8*, *Fgf10* expression is greatly reduced in distal mesenchyme and is barely detectable at later stages (Boulet et al., 2004; Sun et al., 2002). During limb development, *Fgf10* functions to maintain FGFR2b signaling in the AER and the integrity of the AER (Min et al., 1998; Ohuchi et al., 2000; Sekine et al., 1999). This is supported by the observation that after loss of both *Fgf4* and *Fgf8*, there is a higher than normal level of cell death in the AER between E10.5 and E11.5, when *Fgf10* expression is no longer maintained (Boulet et al., 2004; Sun et al., 2002).

As illustrated by *Fgfr2*$^{Msx2-Cre}$ forelimb defects (Fig. 4F), the integrity of the AER is important for maintaining distal mesenchymal proliferation. Therefore, we suggest that after loss of both *Fgf4* and *Fgf8*, distal mesenchymal proliferation is eventually reduced following downregulation of *Fgf10* and premature degeneration of the AER. Thus, in the absence of both *Fgf4* and *Fgf8*, increased mesenchymal cell death results in an initial reduction in limb bud size. The extreme reduction in limb size that occurs by E11.5 is likely to be due to the combined effects of reduced distal mesenchymal proliferation and sustained cell death that result in the complete cessation of limb bud outgrowth.

Continual proliferation of distal mesenchyme is important for distal skeletal element formation. When the AER is excised from chick limb buds at late stages, distal skeletal truncation (loss of autopod elements) correlates with reduced distal mesenchymal proliferation, as mesenchymal cell death no longer occurs after AER removal at late stages of development (Dudley et al., 2002). *Fgfr2*$^{Msx2-Cre}$ forelimb phenotypes further indicate that autopod skeleton formation requires proliferation of distal mesenchymal cells to form a primordium prior to overt morphological changes. The resurgence of autopod skeletal formation after X-irradiation is also likely to be due to restoration of distal mesenchymal proliferation by the intact AER after X-irradiation. Thus, we suggest that distal skeletal defects after loss of both *Fgf4* and *Fgf8* are more likely to be due to reduced mesenchymal proliferation than to increased mesenchymal cell death.

A role for FGF signaling during limb mesenchymal differentiation

As reported previously, disruption of *Fgf8* prior to limb bud initiation results in a limb skeleton that completely lacks the stylopod (Fig. 4C). Formation of the zeugopod and autopod are less affected, presumably owing to increased *Fgf4* expression that maintains some AER-FGF functions (Lewandoski et al., 2000; Moon and Capecchi, 2000). During limb bud development, *Fgf8*

expression precedes that of other AER-FGFs, resulting in a window of time in which only FGF8 is present (from E9.0 to ~E10 in mouse forelimbs). After that, AER-FGF signals comprise FGF8 and other FGFs (FGF4, 9 and 17) (Sun et al., 2000; Sun et al., 2002). In the absence of *Fgf8*, even though *Fgf4* is precociously expressed (Lewandoski et al., 2000), there is still a period of time (from E9.0 to ~E9.75 in mouse forelimbs) when mesenchymal cells fail to receive FGF signals from the AER. This gap in FGF signaling results in stylopod agenesis. Moreover, as shown by *Fgf4/8*$^{Msx2-Cre}$ forelimb phenotypes (Fig. 4D), when mesenchymal cells receive FGF signals during this period of time, stylopod formation proceeds relatively normally and is not affected by extensive proximal cell death or dramatic limb bud size reduction. Thus, stylopod agenesis after loss of *Fgf8* cannot simply be due to reduced mesenchymal cell number, as suggested in previous studies (Lewandoski et al., 2000; Sun et al., 2002).

Previous studies also indicate that loss of AER-FGF signals do not prevent mesenchymal cells from expressing *Sox9*, the earliest marker for chondrogenic differentiation (Akiyama et al., 2002; Wright et al., 1995), but do prevent formation of mesenchymal condensations (Boulet et al., 2004; Sun et al., 2002). Normally, *Sox9* functions to commit undifferentiated mesenchymal cells to osteochondroprogenitors, a cell type that will give rise to both chondrocytes and osteoblasts and to promote mesenchymal condensation formation (Akiyama et al., 2002). During forelimb development, *Sox9* expression begins at E10 in a subpopulation of mesenchymal cells (Akiyama et al., 2005). It is worth noting that at E9.5, prior to *Sox9* expression, AER-FGF-induced MAP kinase activity is already present in the entire forelimb mesenchyme (Corson et al., 2003). Thus, we hypothesize that AER-FGF signals are required for *Sox9*-mediated mesenchymal condensation formation. In support of this hypothesis, previous studies have shown that FGF signaling through the MAP kinase signaling pathway can function synergistically with SOX9 to upregulate *Sox9* expression and that the level of SOX9 protein is critical for the formation of a mesenchymal condensation (Bi et al., 2001; Murakami et al., 2000). Thus, stylopod agenesis after loss of *Fgf8* is not due to reduced mesenchymal cell numbers, but rather to the failure of *Sox9*-expressing cells to undergo further chondrogenic differentiation.

AER-FGF functions during PD pattern formation

During limb skeletal development, prior to initiation of a mesenchymal condensation, some mesenchymal cells undergo initial stages of chondrogenic differentiation, characterized by expression of *Sox9*, but without apparent changes in cell morphology (chondrogenic primordia). Initial *Sox9* expression is localized to central regions of the limb bud, surrounded by undifferentiated mesenchymal cells. Later, the *Sox9* expression domain expands following limb outgrowth, but is still excluded from distal mesenchyme beneath the AER (Akiyama et al., 2005). Owing to the lack of definitive markers for each PD segment at early stages, it is difficult to determine whether the initial *Sox9* expression domain contains progenitors for all three PD segments, or only for the most-proximal segment.

Recent lineage-tracing studies with *Shh-Cre* and the ROSA26 (*R26R*) β-galactosidase reporter suggest that the initial *Sox9* expression domain might not contain progenitors for all three PD segments. Along the PD axis, progeny of *Shh-Cre*-expressing cells are found in the autopod and part of the zeugopod, but never in the stylopod (Harfe et al., 2004). The origin of *Shh-Cre*-expressing cells is limited to the zone of polarizing activity (ZPA) in the posterior

edge of limb mesenchyme, and does not appear to overlap with the central *Sox9* expression domain. This suggests that skeletal lineages in the zeugopod and autopod are not derived from the initial *Sox9* expression domain, but rather are formed at later stages after their progenitors move out of the ZPA. Thus, *Sox9* expression is sequentially regulated along the PD axis, which is consistent with the conclusion that chondrogenic differentiation along the PD axis follows a proximal-to-distal sequence (Summerbell et al., 1973).

We suggest that the initial *Sox9* domain demarcates a chondrogenic primordium for the stylopod, in which *Sox9*-expressing cells only contribute to very proximal skeletal elements. With continual transition of distal undifferentiated cells into *Sox9*-expressing cells, chondrogenic primordia for the zeugopod and autopod become sequentially established (Fig. 4A). During this sequential differentiation process, AER-controlled proliferation provides a source of undifferentiated mesenchymal cells that continually receive AER-FGF signals and progressively differentiate into more-distal skeletal elements. Such a mechanism ensures continual commitment of mesenchymal cells to the osteochondroprogenitors that are essential for mesenchymal condensation formation along the PD axis. This could explain the different skeletal phenotypes in $Fgf8^{RAR-Cre}$ and $Fgf4/8^{Msx2-Cre}$ as well as $Fgfr2^{Msx2-Cre}$ forelimbs, in which AER-FGFs or all AER functions are inactivated at different times during development (Fig. 4C,D,F).

In addition to temporal differences in *Sox9* expression, different PD segments might also regulate *Sox9* expression through distinct molecular mechanisms. This is supported by recent studies of hindlimb phenotypes (lack of the stylopod and zeugopod but normal autopod) in *Gli3* and *Plzf* (also known as *Zbtb16* – Mouse Genome Informatics) double-knockout mice (Barna et al., 2005). In the absence of both *Gli3* and *Plzf*, *Sox9* is not expressed in early limb mesenchyme, which, as we suggest, results in failure of proximal chondrogenic primordia formation and subsequent failure of proximal skeletal element formation. However, owing to normal mesenchymal proliferation and normal *Sox9* expression in distal mesenchymal cells at later stages, autopod chondrogenic primordia and distal skeletal development proceeds normally in mutant hindlimb buds.

In a recent review, after examination of segment-specific marker gene expression, Tabin and Wolpert present ideas that distal proliferation and proximal differentiation are tightly coupled at early stages and that segmental primordia are sequentially established along the PD axis (Tabin and Wolpert, 2007). It is worth noting that establishment of chondrogenic primordia, marked by *Sox9* expression, occurs in a similar timeframe to this PD segmentation process that is defined by segment-specific gene expression. Since, in the absence of *Sox9*, segment-specific genes themselves are insufficient to induce the formation of a mesenchymal condensation (Akiyama et al., 2002), these results suggest that PD skeletal pattern formation requires coordination of chondrogenic- and segment-specific differentiation.

In summary, AER-FGF signals directly or indirectly regulate mesenchymal survival, proliferation and differentiation during limb development. The complete skeletal agenesis after loss of both *Fgf4* and *Fgf8* or all AER functions before limb bud initiation (Fig. 4E,G) is likely to be due to the loss of all of these functions. Finally, in contrast to previous conclusions that AER-FGF signals regulate PD skeletal pattern formation by controlling mesenchymal cell number, our analysis indicates that the AER and AER-FGFs regulate PD skeletal pattern formation through coordinating distal mesenchymal proliferation and chondrogenic differentiation.

References
Akiyama, H., Chaboissier, M. C., Martin, J. F., Schedl, A. and de Crombrugghe, B. (2002). The transcription factor Sox9 has essential roles in successive steps of the chondrocyte differentiation pathway and is required for expression of Sox5 and Sox6. *Genes Dev.* **16**, 2813-2828.
Akiyama, H., Kim, J. E., Nakashima, K., Balmes, G., Iwai, N., Deng, J. M., Zhang, Z., Martin, J. F., Behringer, R. R., Nakamura, T. et al. (2005). Osteo-chondroprogenitor cells are derived from Sox9 expressing precursors. *Proc. Natl. Acad. Sci. USA* **102**, 14665-14670.
Barna, M., Pandolfi, P. P. and Niswander, L. (2005). Gli3 and Plzf cooperate in proximal limb patterning at early stages of limb development. *Nature* **436**, 277-281.
Barrow, J. R., Thomas, K. R., Boussadia-Zahui, O., Moore, R., Kemler, R., Capecchi, M. R. and McMahon, A. P. (2003). Ectodermal Wnt3/beta-catenin signaling is required for the establishment and maintenance of the apical ectodermal ridge. *Genes Dev.* **17**, 394-409.
Bi, W., Huang, W., Whitworth, D. J., Deng, J. M., Zhang, Z., Behringer, R. R. and de Crombrugghe, B. (2001). Haploinsufficiency of Sox9 results in defective cartilage primordia and premature skeletal mineralization. *Proc. Natl. Acad. Sci. USA* **98**, 6698-6703.
Boulet, A. M., Moon, A. M., Arenkiel, B. R. and Capecchi, M. R. (2004). The roles of Fgf4 and Fgf8 in limb bud initiation and outgrowth. *Dev. Biol.* **273**, 361-372.
Corson, L. B., Yamanaka, Y., Lai, K. M. and Rossant, J. (2003). Spatial and temporal patterns of ERK signaling during mouse embryogenesis. *Development* **130**, 4527-4537.
Dudley, A. T., Ros, M. A. and Tabin, C. J. (2002). A re-examination of proximodistal patterning during vertebrate limb development. *Nature* **418**, 539-544.
Eswarakumar, V. P., Monsonego-Ornan, E., Pines, M., Antonopoulou, I., Morriss-Kay, G. M. and Lonai, P. (2002). The IIIc alternative of Fgfr2 is a positive regulator of bone formation. *Development* **129**, 3783-3793.
Eswarakumar, V. P., Lax, I. and Schlessinger, J. (2005). Cellular signaling by fibroblast growth factor receptors. *Cytokine Growth Factor Rev.* **16**, 139-149.
Fallon, J. F., Lopez, A., Ros, M. A., Savage, M. P., Olwin, B. B. and Simandl, B. K. (1994). FGF-2: apical ectodermal ridge growth signal for chick limb development. *Science* **264**, 104-107.
Harfe, B. D., Scherz, P. J., Nissim, S., Tian, H., McMahon, A. P. and Tabin, C. J. (2004). Evidence for an expansion-based temporal Shh gradient in specifying vertebrate digit identities. *Cell* **118**, 517-528.
Hill, T. P., Taketo, M. M., Birchmeier, W. and Hartmann, C. (2006). Multiple roles of mesenchymal beta-catenin during murine limb patterning. *Development* **133**, 1219-1229.
Kmita, M., Tarchini, B., Zakany, J., Logan, M., Tabin, C. J. and Duboule, D. (2005). Early developmental arrest of mammalian limbs lacking HoxA/HoxD gene function. *Nature* **435**, 1113-1116.
Lewandoski, M., Sun, X. and Martin, G. R. (2000). Fgf8 signalling from the AER is essential for normal limb development. *Nat. Genet.* **26**, 460-463.
Lewis, P. M., Dunn, M. P., McMahon, J. A., Logan, M., Martin, J. F., St-Jacques, B. and McMahon, A. P. (2001). Cholesterol modification of sonic hedgehog is required for long-range signaling activity and effective modulation of signaling by Ptc1. *Cell* **105**, 599-612.
Li, C., Xu, X., Nelson, D. K., Williams, T., Kuehn, M. R. and Deng, C. X. (2005). FGFR1 function at the earliest stages of mouse limb development plays an indispensable role in subsequent autopod morphogenesis. *Development* **132**, 4755-4764.
Logan, M., Martin, J. F., Nagy, A., Lobe, C., Olson, E. N. and Tabin, C. J. (2002). Expression of Cre Recombinase in the developing mouse limb bud driven by a Prxl enhancer. *Genesis* **33**, 77-80.
Martin, G. R. (1998). The roles of FGFs in the early development of vertebrate limbs. *Genes Dev.* **12**, 1571-1586.
Min, H., Danilenko, D. M., Scully, S. A., Bolon, B., Ring, B. D., Tarpley, J. E., DeRose, M. and Simonet, W. S. (1998). Fgf-10 is required for both limb and lung development and exhibits striking functional similarity to *Drosophila* branchless. *Genes Dev.* **12**, 3156-3161.
Moon, A. M. and Capecchi, M. R. (2000). Fgf8 is required for outgrowth and patterning of the limbs. *Nat. Genet.* **26**, 455-459.
Murakami, S., Kan, M., McKeehan, W. L. and de Crombrugghe, B. (2000). Up-regulation of the chondrogenic Sox9 gene by fibroblast growth factors is mediated by the mitogen-activated protein kinase pathway. *Proc. Natl. Acad. Sci. USA* **97**, 1113-1118.

Niswander, L. and Martin, G. R. (1993). FGF-4 and BMP-2 have opposite effects on limb growth. *Nature* **361**, 68-71.

Niswander, L., Tickle, C., Vogel, A., Booth, I. and Martin, G. R. (1993). FGF-4 replaces the apical ectodermal ridge and directs outgrowth and patterning of the limb. *Cell* **75**, 579-587.

Ohuchi, H., Nakagawa, T., Yamamoto, A., Araga, A., Ohata, T., Ishimaru, Y., Yoshioka, H., Kuwana, T., Nohno, T., Yamasaki, M. et al. (1997). The mesenchymal factor, FGF10, initiates and maintains the outgrowth of the chick limb bud through interaction with FGF8, an apical ectodermal factor. *Development* **124**, 2235-2244.

Ohuchi, H., Hori, Y., Yamasaki, M., Harada, H., Sekine, K., Kato, S. and Itoh, N. (2000). FGF10 acts as a major ligand for FGF receptor 2 IIIb in mouse multi-organ development. *Biochem. Biophys. Res. Commun.* **277**, 643-649.

Ornitz, D. M. (2000). FGFs, heparan sulfate and FGFRs: complex interactions essential for development. *BioEssays* **22**, 108-112.

Ornitz, D. M. and Itoh, N. (2001). Fibroblast growth factors. *Genome Biol.* **2**, REVIEWS3005.

Ornitz, D. M., Xu, J., Colvin, J. S., McEwen, D. G., MacArthur, C. A., Coulier, F., Gao, G. and Goldfarb, M. (1996). Receptor specificity of the fibroblast growth factor family. *J. Biol. Chem.* **271**, 15292-15297.

Orr-Urtreger, A., Givol, D., Yayon, A., Yarden, Y. and Lonai, P. (1991). Developmental expression of two murine fibroblast growth factor receptors, *flg* and *bek*. *Development* **113**, 1419-1434.

Revest, J. M., Spencer-Dene, B., Kerr, K., De Moerlooze, L., Rosewell, I. and Dickson, C. (2001). Fibroblast growth factor receptor 2-IIIb acts upstream of Shh and Fgf4 and is required for limb bud maintenance but not for the induction of Fgf8, Fgf10, Msx1, or Bmp4. *Dev. Biol.* **231**, 47-62.

Rowe, D. A. and Fallon, J. F. (1982). The proximodistal determination of skeletal parts in the developing chick leg. *J. Embryol. Exp. Morphol.* **68**, 1-7.

Rowe, D. A., Cairns, J. M. and Fallon, J. F. (1982). Spatial and temporal patterns of cell death in limb bud mesoderm after apical ectodermal ridge removal. *Dev. Biol.* **93**, 83-91.

Saunders, J. W. (1948). The proximo-distal sequence of the origin of the parts of the chicken wing and the role of the ectoderm. *J. Exp. Zool.* **108**, 363-404.

Sekine, K., Ohuchi, H., Fujiwara, M., Yamasaki, M., Yoshizawa, T., Sato, T., Yagishita, N., Matsui, D., Koga, Y., Itoh, N. et al. (1999). Fgf10 is essential for limb and lung formation. *Nat. Genet.* **21**, 138-141.

Summerbell, D. (1974). A quantitative analysis of the effect of excision of the AER from the chick limb-bud. *J. Embryol. Exp. Morphol.* **32**, 651-660.

Summerbell, D., Lewis, J. H. and Wolpert, L. (1973). Positional information in chick limb morphogenesis. *Nature* **244**, 492-496.

Sun, X., Lewandoski, M., Meyers, E. N., Liu, Y. H., Maxson, R. E., Jr and Martin, G. R. (2000). Conditional inactivation of Fgf4 reveals complexity of signalling during limb bud development. *Nat. Genet.* **25**, 83-86.

Sun, X., Mariani, F. V. and Martin, G. R. (2002). Functions of FGF signalling from the apical ectodermal ridge in limb development. *Nature* **418**, 501-508.

Tabin, C. and Wolpert, L. (2007). Rethinking the proximodistal axis of the vertebrate limb in the molecular era. *Genes Dev.* **21**, 1433-1442.

Trokovic, R., Trokovic, N., Hernesniemi, S., Pirvola, U., Vogt Weisenhorn, D. M., Rossant, J., McMahon, A. P., Wurst, W. and Partanen, J. (2003). FGFR1 is independently required in both developing mid- and hindbrain for sustained response to isthmic signals. *EMBO J.* **22**, 1811-1823.

Verheyden, J. M., Lewandoski, M., Deng, C., Harfe, B. D. and Sun, X. (2005). Conditional inactivation of Fgfr1 in mouse defines its role in limb bud establishment, outgrowth and digit patterning. *Development* **132**, 4235-4245.

Wang, C. K., Omi, M., Ferrari, D., Cheng, H. C., Lizarraga, G., Chin, H. J., Upholt, W. B., Dealy, C. N. and Kosher, R. A. (2004). Function of BMPs in the apical ectoderm of the developing mouse limb. *Dev. Biol.* **269**, 109-122.

Wolpert, L., Tickle, C. and Sampford, M. (1979). The effect of cell killing by x-irradiation on pattern formation in the chick limb. *J. Embryol. Exp. Morphol.* **50**, 175-193.

Wright, E., Hargrave, M. R., Christiansen, J., Cooper, L., Kun, J., Evans, T., Gangadharan, U., Greenfield, A. and Koopman, P. (1995). The Sry-related gene Sox9 is expressed during chondrogenesis in mouse embryos. *Nat. Genet.* **9**, 15-20.

Yamaguchi, T. P., Bradley, A., McMahon, A. P. and Jones, S. (1999). A Wnt5a pathway underlies outgrowth of multiple structures in the vertebrate embryo. *Development* **126**, 1211-1223.

Yu, K., Xu, J., Liu, Z., Sosic, D., Shao, J., Olson, E. N., Towler, D. A. and Ornitz, D. M. (2003). Conditional inactivation of FGF receptor 2 reveals an essential role for FGF signaling in the regulation of osteoblast function and bone growth. *Development* **130**, 3063-3074.

Zhang, X., Ibrahimi, O. A., Olsen, S. K., Umemori, H., Mohammadi, M. and Ornitz, D. M. (2006). Receptor specificity of the fibroblast growth factor family. The complete mammalian FGF family. *J. Biol. Chem.* **281**, 15694-15700.